



HAL
open science

Minimal Parameter Formulations Dynamic Traffic Assignment using the Macroscopic Fundamental Diagram: Freeway vs City Streets User Equilibrium revisited

Jorge A Laval, Ludovic Leclercq, Ludovic Chiabaut

► **To cite this version:**

Jorge A Laval, Ludovic Leclercq, Ludovic Chiabaut. Minimal Parameter Formulations Dynamic Traffic Assignment using the Macroscopic Fundamental Diagram: Freeway vs City Streets User Equilibrium revisited. 22nd International Symposium on Transportation and Traffic Theory (ISTTT22), Jul 2017, Evanston IL, United States. pp.517-530, 10.1016/j.trpro.2017.05.029 . hal-01590473

HAL Id: hal-01590473

<https://hal.science/hal-01590473>

Submitted on 19 Sep 2017

HAL is a multi-disciplinary open access archive for the deposit and dissemination of scientific research documents, whether they are published or not. The documents may come from teaching and research institutions in France or abroad, or from public or private research centers.

L'archive ouverte pluridisciplinaire **HAL**, est destinée au dépôt et à la diffusion de documents scientifiques de niveau recherche, publiés ou non, émanant des établissements d'enseignement et de recherche français ou étrangers, des laboratoires publics ou privés.

Minimal Parameter Formulations of the Dynamic User Equilibrium using Macroscopic Urban Models: Freeway vs City Streets Revisited

Jorge A. Laval^{a,*}, Ludovic Leclercq^b, Nicolas Chiabaut^b

^aSchool of Civil and Environmental Engineering, Georgia Institute of Technology

^bLaboratoire Ingénierie Circulation Transport, IFSTTAR, ENTPE, Univ. Lyon

Abstract

This paper investigates the dynamic user equilibrium (DUE) on a single origin-destination pair with two alternative routes, a freeway with a fixed capacity and the surrounding city-streets network, modeled with a network macroscopic fundamental diagram (NMFD). We find using suitable transformations that only a single network parameter is required to characterize the DUE solution, the freeway to NMFD capacity ratio. We also show that the stability and convergence properties of this system are captured by the constant demand case, which corresponds to an autonomous dynamical system that admits analytical solutions. This solution is characterized by two critical accumulation values that determine if the steady state is in free-flow or gridlock, depending on the initial accumulation. Additionally, we also propose a continuum approximation to account for the spatial evolution of congestion, by including variable trip length and variable NMFD coverage area in the model. It is found that gridlock cannot happen and that the steady-state solution is independent of surface network parameters. These parameters do affect the rate of convergence to the steady-state solution, but convergence rates appear virtually identical when time is expressed in units of the NMFD free-flow travel time.

© 2016 The Authors. Elsevier B.V. All rights reserved. Peer review under responsibility of the scientific committee of the 22nd International Symposium on Transportation and Traffic Theory.

Keywords: dynamic traffic assignment, macroscopic fundamental diagram

1. Introduction

The simplest models that incorporate the effects of congestion on urban areas are reservoir models. They are based on vehicle conservation inside the reservoir with its outflow given by a known function of the accumulation. This function, called the Network Macroscopic Fundamental Diagram (NMFD), was first introduced in Godfrey (1969) and later used by Mahmassani et al. (1984, 1987), but only recently was shown to have strong empirical support suggesting a rather stable shape Daganzo (2007); Geroliminis and Daganzo (2007); Wang et al. (2015). Many control applications have been proposed since (e.g., Haddad and Geroliminis, 2012; Aboudolas and Geroliminis, 2013; Ampountolas et al., 2014; Hajiahmadi et al., 2013; Knoop and Hoogendoorn, 2014; Yildirimoglu et al., 2015; Kouvelas et al., 2016).

Apart from the shape of the NMFD, the main assumption of a reservoir model is that the travel time of a vehicle entering at time t is a function of the accumulation at the same time, which makes it applicable only when the inflow varies slowly. Otherwise it may be subject to the “infinite-wave-speed problem” due to the lack of a space dimension in the model. Thus, when fast inflow variations occur, they have immediate repercussions on the outflow meaning that information travel is infinitely fast inside the reservoir. Improved reservoir models have been proposed that guaranty that all vehicles travel their trip length before exiting (Arnott, 2013; Fosgerau, 2015; Lamotte and Geroliminis, 2016;

Mariotte et al., 2017) at the expense of mathematical tractability. But when demand varies slowly, the simple reservoir gives good approximations, with the big advantage of being analytical. This has allowed extensions such as congestion pricing (Arnott, 2013; Daganzo and Lehe, 2015).

This paper focuses on the simple reservoir model in the context of dynamic traffic assignment (DTA), in particular the dynamic user equilibrium (DUE) when there is the alternative of reaching the destination using a freeway of limited capacity. Although there have been efforts in the past to combine DTA and MFD (Yildirimoglu and Geroliminis, 2014a; Leclercq and Geroliminis, 2013), existing methods are algorithmic or numerical. Apart from the numerical errors introduced, this approach makes it difficult to answer fundamental questions such as: (i) what are the parameters, or combinations thereof, that affect the solution? (ii) under what conditions is the simple reservoir model a good approximation? (iii) will the system converge to gridlock and how fast?

To answer these and other questions, here we establish the minimum set of parameters needed to fully characterize the DUE solution. Towards this end, section 2 considers the simplest problem of a single NMFD (no DUE) to show that the accumulation evolution is characterized by two critical accumulation values that determine if the steady state is in free-flow or gridlock, depending on the initial accumulation. It also shows that the stability and convergence properties of this system are captured by the constant demand case, which admits analytical solutions. Section 3 shows that only a single network parameter is required to characterize the DUE solution, the freeway to NMFD capacity ratio. Section 4 proposes a continuum approximation to account for the spatial evolution of congestion, by including variable trip length and variable NMFD coverage area, typically assumed constant in the literature (e.g., Haddad and Geroliminis, 2012; Aboudolas and Geroliminis, 2013; Hajiahmadi et al., 2013; Leclercq et al., 2015; Yildirimoglu and Geroliminis, 2014b). Finally section 5 presents a discussion.

2. Single NMFD loading

We start by considering the simplest problem of the dynamic loading of a surface network using a single NMFD; there is no freeway alternative, and therefore no DUE. It turns out that the solution to this problem is the building block for the following sections.

We assume that the surface network can be well described by an outflow-NMFD, $f(n)$, with capacity $\mu \equiv \max_n f(n)$. This function gives the production, i.e. the number of trip completions per unit time, as a function of the number of vehicles in the network, n . Let $\lambda(t)$ be the demand inflow into the network at time t .¹ The NMFD dynamics studied in this paper are given by the following ordinary differential equation (ODE):

$$\mathbf{n\text{-ODE:}} \begin{cases} n'(t) = \lambda(t) - f(n), & \text{(reservoir dynamics)} & (1a) \\ n(0) = n_0, & \text{(initial conditions)} & (1b) \end{cases}$$

where primes denote differentiation, $\lambda(t)$ the inflow and n_0 specify the initial conditions. A key point is whether or not demand is restricted by the supply function of the NMFD, Ω ; i.e.,

$$\lambda(t) \leq \Omega(n(t)). \quad \text{(supply constraint)} \quad (2)$$

Although this appears to be a standard assumption in the latest literature, we argue that this constraint negates the fact that distance traveled within the reservoir may increase with congestion. Therefore, we are interested here in the *unconstrained* system solution. We will show how solutions to the constrained system can be derived from the solutions presented here.

It is convenient to express system dynamics in terms of the dimensionless variables occupancy, $k(t)$, and demand intensity $\rho(t)$:

$$k(t) \equiv n(t)/(\kappa L), \quad 0 \leq k(t) \leq 1, \quad \text{(occupancy)} \quad (3a)$$

$$\rho(t) \equiv \lambda(t)/\mu, \quad \text{(demand intensity)} \quad (3b)$$

¹ The word “demand” is used in the traffic flow context to distinguish the willingness to traverse a bottleneck (demand) from the ability to do so (flow); it is not used in the economics context to reflect cost elasticity. Here, the demand is an inelastic and exogenous time-dependent function.

where κ is the jam density for one lane, assumed identical for all lanes in the network, and L corresponds to the length of the network, such that κL is the maximum number of bumper-to-bumper vehicles inside the NMFd coverage area. We assume a general speed-occupancy NMFd, $V_k(k)$, of the form:

$$V_k(k) = ug(k), \tag{MFD speed-occupancy} \tag{4}$$

where u is the NMFd free-flow speed (which is \leq FD free-flow speed as it includes the effects of signals) and $g(k)$ is an arbitrary function of the occupancy satisfying $g(0) = 1, g(1) = 0$ and $g' < 0$. The speed-accumulation NMFd, $V(n)$, and the $f(n)$ can be derived as follows (Daganzo, 2007):

$$V(n) = V_k(n/(\kappa L)), \tag{MFD speed-accumulation} \tag{5a}$$

$$f(n) = V(n) n/\ell = g(n/(\kappa L))nu/\ell, \tag{outflow-MFD} \tag{5b}$$

where ℓ is the trip length, assumed identical for all commuters.

The key observation here is that ℓ and u can be eliminated from the formulation by noting that the free-flow travel time inside the NMFd coverage area, namely $\tau^* \equiv \ell/u$, corresponds to the timescale of our problem, and that therefore it can be eliminated by rescaling time. To see this, (i) let $\hat{t} \equiv t/\tau^*$ be the rescaled time, so that demand becomes $\rho(\hat{t}) = \rho(t/\tau^*)$, and (ii) express the NMFd capacity as $\mu \equiv \kappa Lc/\tau^*$ for some positive constant c . This constant is the single supply parameter needed in this formulation and defines the ‘‘shape’’ of the NMFd, e.g. $c = 1/4$ for parabolic and $c = 1/2$ for isosceles $f(k)$. Dividing (1) by κL and using (3a) gives that in original time the occupancy ODE of the system can be expressed as:

$$\mathbf{k}\text{-ODE: } \begin{cases} k'(t) = F(t/\tau^*, k)/\tau^*, & \text{(reservoir dynamics)} & \tag{6a} \\ F(t/\tau^*, k) \equiv c\rho(t/\tau^*) - kg(k), & & \tag{6b} \\ k(0) = k_0, & \text{(initial conditions)} & \tag{6c} \end{cases}$$

where $F(t/\tau^*, k)$ is an auxiliary function. It follows from the chain rule that in rescaled time (6a) becomes $k'(\hat{t}) = F(\hat{t}, k)$, which is independent of τ^* . Hence, hereafter we will analyze the solution of

$$\mathbf{k}\text{-ODE: } \begin{cases} k'(t) = F(t, k), & \text{(reservoir dynamics)} & \tag{7a} \\ F(t, k) \equiv c\rho(t) - kg(k), & & \tag{7b} \\ k(0) = k_0, & \text{(initial conditions)} & \tag{7c} \end{cases}$$

where we have dropped the hat for clarity (and from now on). Notice that this rescaling eliminates τ^* regardless of the shape of both $g(k)$ and $\rho(t)$, which are the only parameters involved in our problem. As shown next, however, an additional transformation can be applied to time and space to justify a linear parameter-less function for $g(x)$.

2.1. A Greenshield approximation

It has been shown (Laval and Castrillon, 2015; Daganzo and Knoop, 2016; Laval and Chilukuri, 2016) that in the context of the Kinematic Wave model (Lighthill and Whitham, 1955; Richards, 1956) with triangular FD for road segments, under a set of linear transformations of flow, occupancy, space and time, individual delays (and other measures of performance) are invariant. This means that individual vehicular delays remain the same regardless of the parameters in the transformation. As argued in Laval and Castrillon (2015) this can be used to streamline calculations by choosing the FD that simplifies the problem the most. In particular, they showed that for an isosceles triangle FD the resulting network NMFd becomes smooth and symmetric with respect to the y-axis. This gives the strong indication that a parabolic NMFd should a good approximation, which here means that:

$$g(k) \equiv 1 - k. \tag{Greenshield approximation} \tag{8}$$

The NMFd capacity becomes $\mu = f(\kappa L/2) = u\kappa L/\ell/4 = \kappa L/(4\tau^*)$, which means that $c = 1/4$. Model (8) will be assumed at some point in each section below.

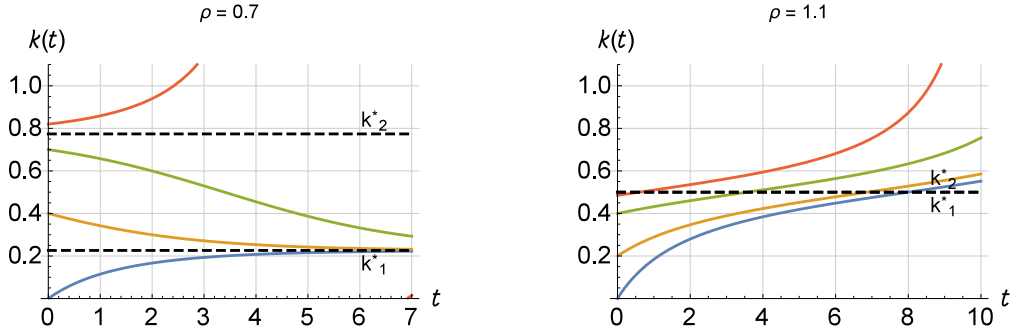


Fig. 1. Single NMF loading, constant demand case. Illustration of the analytical solution (12), which depends on the single parameter ρ . Recall that t is measured in units of τ^*

2.2. Analytical solutions

The ODE (7) (or (1)) cannot be solved analytically for general $\rho(t)$ and $g(k)$. However, when demand is constant, i.e. $\rho(t) = \rho$, then $F(t, k) = F(k) = c\rho - kg(k)$. In this case (7) is said to be an *autonomous system* since its evolution depends only on the occupancy and not on other time-dependent functions. Autonomous dynamical systems are well understood (see e.g. Teschl, 2010), and despite their simplicity, they capture most of the dynamics under more general demand patterns in our case.

In the case of traffic flow, the solution of these systems is fully characterized by two critical occupancies that are the roots of $F(k^*) = 0$: one in free-flow, k_1^* , and another in congestion, k_2^* ; see Fig. 3 (inset). Since $F'(k_1^*) < 0$ and $F'(k_2^*) < 0^2$ it follows that k_1^* is stable (attractor) and k_2^* unstable (repellor). This means that initial conditions “close to” k_1^* will tend to k_1^* as $t \rightarrow \infty$, and that initial conditions close to k_2^* will diverge away either to k_1^* or to gridlock.

Under the Greenshield approximation we have:

$$k_1^* = (1 - \sqrt{1 - \rho})/2, \quad (\text{attractor}) \quad (9a)$$

$$k_2^* = (1 + \sqrt{1 - \rho})/2, \quad (\text{repellor}) \quad (9b)$$

Note that ρ is the single parameter that describes the system.

The solution of autonomous dynamical systems can be obtained by the standard techniques for separable ODEs. In our case, we write (7) as $dk/F(k) = dt$ and integrate to obtain $t = T(k) - T(k_0)$, where $T(k) = \int dk/F(k)$. This gives:

$$k(t) = T^{-1}(T(n_0) + t), \quad (\text{autonomous case solution}) \quad (10)$$

It can be shown that in our case:

$$T(k) = \frac{1}{c_1} \tanh^{-1} \left(\frac{1/2 - k}{c_1} \right), \quad (11)$$

with $c_1 = \sqrt{1 - \rho}/2$, and thus the solution (10) can be expressed as:

$$k(t) = 1/2 - c_1 \tanh(T(k_0) + c_1 t). \quad (\text{autonomous, Greenshield solution}) \quad (12)$$

Fig. 1 shows the occupancy $k(t)$ for 4 initial values $k_0 = k(0)$ and 2 values for ρ . We can see that (i) when $\rho \leq 1$ then $k \rightarrow k_1^*$ if $k_0 \leq k_2^*$ and to 1 (gridlock) if $k_0 > k_2^*$, as expected, (ii) the convergence to gridlock happens at an increasing rate, (iii) the relaxation time of the system is comparable to $5\tau^*$ in most cases, (iv) when $\rho > 1$, i.e. when the demand exceeds the MFD capacity, the system converges to gridlock for all initial occupancies, as expected because the inflow is unrestricted.

² Since $F'(k^*) = (k^* g(k^*))'$ corresponds to the wave speed of the k-MFD.

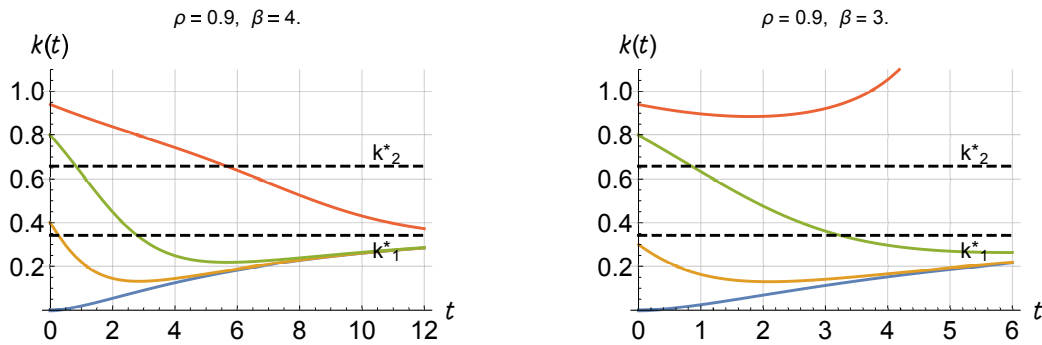


Fig. 2. Single NMF loading, exponential demand case, given by (13a) with $q_0 = 0, \rho = q_1/\mu = 0.9$, for 4 initial values $k_0 = \{0, .3, .8, .94\}$, and for 2 different β values. Notice that for $k_0 = 0.94$ the steady-state solution is different for different values of β .

2.2.1. Rush-hour demand patterns

We have been able to find analytical solutions for a family of demand curves well suited to model rush-hour periods, but only under the Greenshield approximation. These include second degree polynomial, exponential, and logistic functions. In particular, consider the following demand functions:

$$\lambda(t) \equiv q_0 + [1 - \exp(-t/t^*)](q_1 - q_0), \tag{exponential} \tag{13a}$$

$$\lambda(t) \equiv q_0 + [1 + \exp(-t/t^*)]^{-1}(q_1 - q_0), \tag{logistic} \tag{13b}$$

where q_0 and q_1 are the initial and final demand flows, respectively, and t^* is the time scale, which regulates how fast this transition takes place and which could be measured by fitting the appropriate functional form to empirical data. Since $e^{-4} \approx 0$ we can say that the relaxation time is $\approx 4t^*$ for exponential and $\approx 8t^*$ for logistic demands.

The analytical solutions (produced with mathematical software) are too lengthy in general to include here; a few simple examples are included in the appendix. The important point is that (i) these solutions can be evaluated with arbitrary precision, even under a time-varying demand, and (ii) in the case of the rush-hour patterns considered here, at most two dimensionless parameters are needed to evaluate $k(t)$ if time is measured in units of τ^* :

$$\rho \equiv q_1/\mu, \tag{steady-state intensity} \tag{14a}$$

$$\beta \equiv t^*/\tau^*, \tag{time scale ratio} \tag{14b}$$

The parameter ρ is now the steady-state intensity, which should be ≤ 1 if (2) is assumed. The significance of the β parameter is that it can be used to discern when model (1) is a good approximation. To see this, note that time scale of NMF dynamics (or relaxation time) should be comparable to the average trip time, which should be a small multiple of τ^* , and we have already noted that the demand time scale is proportional to t^* . It follows that β is proportional to the ratio of demand and supply time scales. The constant of proportionality depends on the type of demand function, but in general large values of β indicate that the demand varies slowly compared to the speed at which the MFD converges to equilibrium.

For these more general demand patterns we found that the solution is qualitatively very similar to the autonomous case where $\lambda(t) = q_1$. This is as expected because in the steady-state, demands (13) are constant (and equal to q_1). The main difference is in the transition to the steady-state solution, in particular the initial value above which the system tends to gridlock, which equals k_2^* in the autonomous case, but here it depends on β ; see Fig. 2.

It is important to remember that when the supply constraint (2) is active, the solution changes such that gridlock is impossible: if $k_0 > k_2^*$ then $k(t) = k_0$, else $k(t)$ tends to k_1^* exponentially.

3. Freeway bottleneck vs NMF

In this section we add a freeway as an alternative to the city street network (CS) modeled as in the previous section. It is generally agreed that freeways cannot be well approximated with an MFD because of the infinite-wave-speed

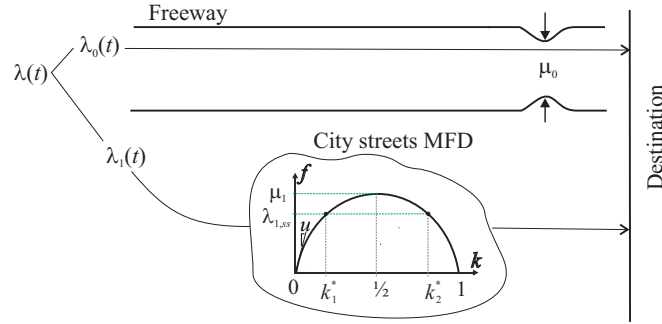


Fig. 3. Freeway vs CS network: constant network length model.

problem and hysteresis loops (Saberi and Mahmassani, 2013; Mahmassani et al., 2013; Geroliminis and Sun, 2011; Leclercq et al., 2014). In this section we present the results for the UE between a freeway, modeled as a bottleneck of capacity μ_0 , and the CS, modeled with an NMFD, $f(n)$, of capacity μ_1 and with constant network length, L , per the previous section; see Fig. 3. In general, the subindex $i=0$ will be used for freeway and $i = 1$ for the CS, except for CS-only variables, where it will be omitted.

We consider here the following system dynamics:

$$\tau_0(t) = \tau_0^* + w_0(t), \quad (\text{freeway travel time}) \quad (15a)$$

$$\tau_1(t) = n(t)/f(n(t)), \quad (\text{CS travel time}) \quad (15b)$$

$$n'(t) = \lambda_1(t) - f(n(t)), \quad (\text{reservoir dynamics}) \quad (15c)$$

$$\lambda(t) = \lambda_0(t) + \lambda_1(t), \quad (\text{demand conservation}) \quad (15d)$$

where $\lambda_i(t)$ denotes the demand flow to each route, $\tau_1^* \equiv \ell/u$ is the free-flow CS travel time, and $w_0(t)$ is the freeway queuing delay, which is given by $w_0(t) = A_0(t)/\mu_0 - t \geq 0$; see Laval (2009). As in this reference, we set $t = 0$ when travel times are identical on both alternatives; i.e., $\tau_0(0) = \tau_1(0)$. This enables us to use the UE condition in differential form for $t \geq 0$, which equalizes the rate of change in travel times: $\tau_0'(t) = \tau_1'(t)$, with $\tau_0'(t) = \lambda_0(t)/\mu_0 - 1$ and $\tau_1'(t) = (1 - nf'/f)n'/f$. This gives:

$$\lambda_0(t) = (1 + \tau_1'(t))\mu_0, \quad (\text{differential UE condition}) \quad (16a)$$

$$= (1 + (1 - nf'/f)n'/f)\mu_0. \quad (16b)$$

Combining (15d), (15c) and (16) to eliminate λ_1 gives the ODE describing system dynamics:

$$\text{UE-ODE: } \begin{cases} n'(t) = \frac{(\lambda - \mu_0 - f)f}{(1 - nf'/f)\mu_0 + f} \\ n(0) = n_0, \end{cases} \quad (17a)$$

$$(17b)$$

which is an explicit nonlinear first-order ODE of degree 1, and is valid for $t \geq 0$. Unfortunately, (17) does not admit an explicit analytical solution without specifying $\lambda(t)$ and $f(t)$. However, one can still extract valuable insight. In particular, one can see that:

(i) the equilibrium travel time $\tau(t)$ increases with n' . To see this, notice that $\tau'(t) = (1 - nf'/f)n'/f$ and that

$$1 - nf'/f \geq 0, \quad (18)$$

for concave NMFDs.

(ii) a steady-state accumulation is reached when $n'(t) = 0$, i.e. when $\lambda - \mu_0 - f = 0$. It follows that, qualitatively, the steady-state solution in this section is similar to the single NMFD loading problem, which is characterized by two critical accumulations (one attractor and one repeller) that are the roots of $f(n^*) = \lambda - \mu_0$.

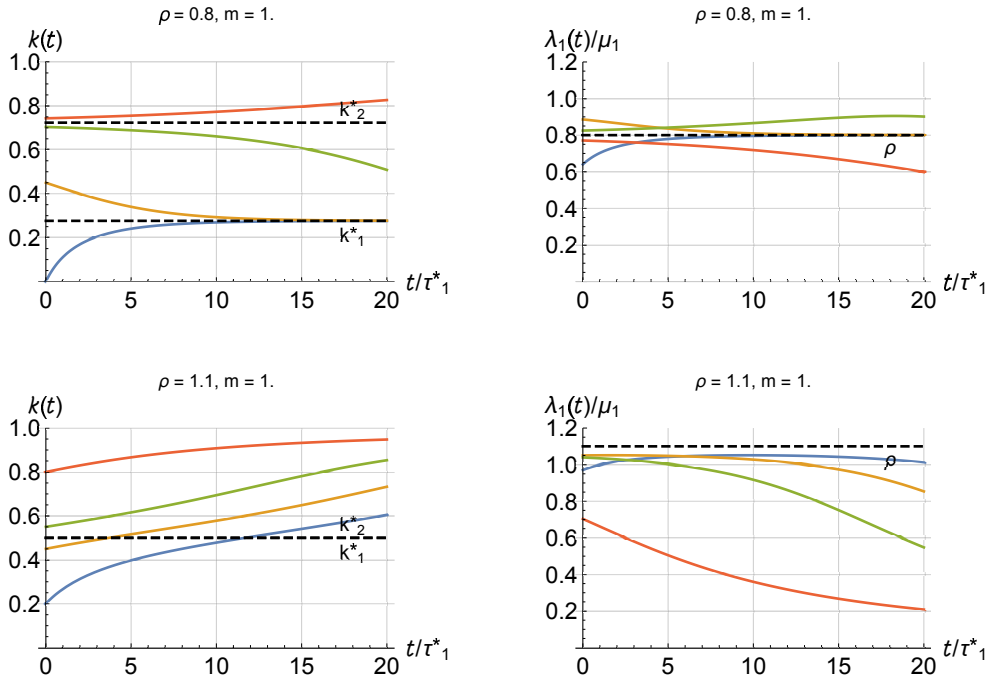


Fig. 4. Freeway vs MFD, constant network length model. Occupancy $k(t)$ and the resulting CS inflow $\lambda_1(t)$ for 4 initial values $k_0 = k(0)$, and for different ρ, m values.

(iii) the flow diverted to the CS network as function of n can be obtained combining (15c) and (17a), which gives:

$$\lambda_1(t, n) = \frac{\lambda - \mu_0 n f' / f}{1 + (1 - n f' / f) \mu_0 / f} \tag{19}$$

This expression indicates that: (a) diversion always takes place as both the numerator and denominator in (19) are always positive. This is a consequence of (18) and of $\lambda > \mu_0$ (recall that congestion in the CS can only happen if the freeway is already congested), (b) at the CS capacity, $f' = 0$ and thus $\lambda_1 = \lambda \mu_1 / (\mu_0 + \mu_1)$ is a constant. This diversion pattern was called diversion type-2 in Laval (2009) who modeled the CS as a bottleneck: the total demand is split proportionally to each alternative’s capacity, (d) the limit of λ_1 as $n \rightarrow L\kappa$ is always zero, and the limit of λ_1 as $n \rightarrow 0$ is always positive, but depends on the NMF, e.g., a linear free-flow branch gives $\lambda - \mu_0$.

3.1. Analytical solutions

It turns out that the problem in this section can also be expressed as $k'(t) = F(t, k) / \tau_1^*$. The derivation is similar to that of (6); divide (17) by κL , use (3a) and (5). This means that the parameter τ_1^* can be eliminated by rescaling time, and that one may solve the simplified problem:

$$\mathbf{k\text{-UE-ODE}}: \begin{cases} k'(t) = F(t, k), & \text{(reservoir dynamics)} & (20a) \\ F(t, k) \equiv \frac{c\rho(t) - kg}{1 - cmg' / g^2}, & & (20b) \\ k(0) = k_0, & \text{(initial conditions)} & (20c) \end{cases}$$

where t is measured in units of τ_1^* , and the dimensionless parameters m and ρ are given by:

$$m = \mu_0 / \mu_1, \tag{21a} \text{ (capacity ratio)}$$

$$\rho(t) \equiv (\lambda(t) - \mu_0) / \mu_1 = \lambda(t) / \mu_1 - m, \tag{21b} \text{ (MFD demand intensity)}$$

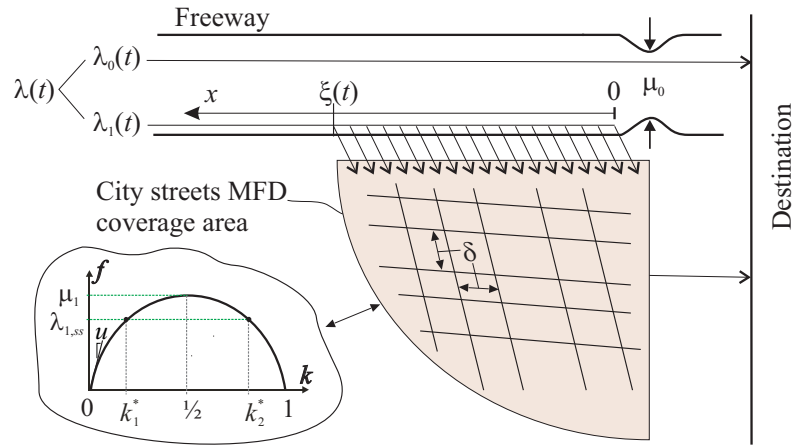


Fig. 5. Freeway vs CS network: variable network length model.

Notice how as $m \rightarrow 0$ (no freeway) then ODE (20) \rightarrow ODE (7), and therefore the solution to the single MFD loading problem in section 2 is a special case of the solution in this section. Unfortunately, unlike section 2, we were not able to find analytical solutions for ODE (20) under any time-dependent demand $\rho(t)$. The autonomous case $\rho(t) = \rho$, however, can still be solved analytically, and it turns out that the solution has a lot in common with the single NMFDF case: we have the same two critical occupancies, k_1^* and k_2^* , with the same stability properties as given by (9). To see this, it is clear from (20b) that the solution of $F(k^*) = 0$ is still given by (9); for the stability properties, one can verify that $F'(k^*)$ is proportional to $-(k^{*2}g'(k^*) - c\rho)$, which can be written as $k^*(k^*g(k^*))'$. This expression is proportional to the wave speed $(k^*g(k^*))'$ and the conclusion follows.

Therefore, the solution of (20) in the autonomous case $\rho(t) = \rho$ is also given by (10), which depends upon the shape of the MFD. Under the Greenshield approximation we obtain $F(k) = (\rho - 4(1-k)k)/(4 + m/(1-k)^2)$, and $T(k) = \int dk/F(k)$ is given by :

$$T(k) = \left(1 + (2 - \rho)m/\rho^2\right)T^1(k) + \frac{m}{\rho^2} \left(\frac{\rho}{1-k} + 2 \log \left(\frac{\rho - 4(1-k)k}{(1-k)^2} \right) \right) \quad (22)$$

where $T^1(k)$ is the corresponding T -function for the single NMFDF loading problem, given by (11). Again, as $m \rightarrow 0$ (no freeway) then $T \rightarrow T^1$ and therefore the solution to the single MFD loading problem is a special case of the solution in this section. Similarly, as $m \rightarrow \infty$ (no CS) then $T \rightarrow \infty$, which means that the CS will never be used.

Fig. 4 shows the occupancy $k(t)$ given by (10)-(22) and the resulting CS inflow $\lambda_1(t)/\mu_1$ for 4 initial values $k_0 = k(0)$, and for different ρ, m values. As mentioned earlier, we can see that the evolution of the system is very similar to single NMFDF case in Fig. 1, and therefore the same conclusions apply here. The main differences are that (i) the convergence to gridlock happens at a decreasing (rather than increasing) rate, and (ii) the relaxation time of the system might be larger. Notice the demand patterns produced in the CS are not time-independent (as one might have expected from an autonomous case). In fact they appear to be exponential for free-flow initial conditions, and logistic or bell-shaped for congested initial conditions.

4. A continuum approximation for off-ramps

In this section we combine the formulation proposed in the previous sections with the continuum approximation (CA) proposed in Laval (2009). In this approximation, the set of discrete off-ramps is treated as a continuum, where vehicles can exit the freeway at any given location $x \geq 0$ upstream of a freeway bottleneck located at $x = 0$. They show that when the CS speed is constant the UE solution is characterized by an “information wave”, $\xi(t)$, that marks

the most upstream location where vehicles divert; i.e., vehicles divert in $0 \leq x \leq \xi(t)$. Assuming a constant lateral exit capacity, ϕ , in units of vehicles / (time×distance), the total lateral diverting flow at time t , $\lambda_1(t)$, can be expressed as:

$$\lambda_1(t) = \phi\xi(t). \tag{23}$$

Here, the CS speed is given by the NMFDF over a coverage area that increases (quadratically) with $\xi(t)$.

To illustrate, let δ be the average distance between two parallel and consecutive streets as in Fig. 5. The number of blocks inside a coverage area A is then A/δ^2 , each contributing 2δ to the network length, assuming that only southbound and eastbound links will be used. Taking an area given by a quarter-disk of radius $\xi(t)$, gives that the network length can be expressed as:

$$L(\xi) = \frac{\pi\xi^2}{2\delta}, \tag{24}$$

We assume that the trip length is proportional to the network length, i.e. that:

$$\gamma \equiv L/\ell \tag{25}$$

is a constant. With all, system dynamics are identical to the previous section, except that now there are two unknown functions, $n(t)$ and $\xi(t)$; i.e.:

$$\begin{cases} \lambda(t) = (\tau_1'(t) + 1)\mu_0 + \phi\xi(t), & (26a) \\ n'(t) = \phi\xi(t) - f(n(t), \xi(t)) & (26b) \\ (n(0), \xi(0)) = (n_0, \xi_0), & (26c) \end{cases}$$

where $n_0 < \kappa L(\xi_0)$ has to be imposed so that the initial accumulation does not exceed jam accumulation, and $f(n, \xi)$ is given by (8) with $L = L(\xi)$ and $\ell = \ell(\xi)$, as prescribed in this section.

It can be verified that in steady-state we have the following equilibrium values:

$$\lambda_{1,ss} = \lambda_{ss} - \mu_0, \quad \xi_{ss} = \frac{\lambda_{1,ss}}{\phi}, \quad \ell_{ss} = \frac{\pi\xi_{ss}^2}{4\gamma\delta}, \quad L_{ss} = \ell_{ss}\gamma, \quad \mu_{1,ss} = \frac{1}{4}\gamma\kappa u_1, \quad \tau_{1,ss}^* = \frac{\ell_{ss}}{u_1}. \tag{27}$$

where the subscript "ss" means the steady-state of the variable, e.g. $\xi_{ss} \equiv \xi(t \rightarrow \infty)$. The two critical occupancy values k_1^* and k_2^* are still given by (9) with $\rho = \lambda_{1,ss}/\mu_{1,ss}$. Notice that the steady-state location of the information wave, ξ_{ss} , is independent of the supply parameters on the CS, and it is only a function of the steady-state demand and the exit capacity. This means, for example, that the free-flow speed, or the number of lanes on the CS facilities does not affect the solution for large times. These parameters do affect the rate of convergence to the steady-state solution, as shown next.

Unfortunately, we were not able to find analytical solutions even for the Greenshield approximation under constant demand, and therefore we resort to numerical methods. Fig. 6 shows the evolution of various quantities of interest for problem in the case of a constant demand $\lambda(t) \equiv q$ for 4 different free-flow CS speed u_1 , and for empty CS initial conditions $\xi_0 = 0^+$, $n_0 = 0$ (a very small value 0^+ is needed since the NMFDF has to cover a nonzero area).

The first column in the figure uses regular units, while the second uses the dimensionless forms from the last section to express the of convergence to steady-state values measuring time in units of τ_1^* . The main result of this figure is the low scatter observed for the solution $n(t)$, $\xi(t)$ in the dimensionless form. This means that the solution to our problem can be cast independently of the CS free-flow speed u_1 . Also, we have verified that $k_{ss} \rightarrow k_1^*$ if $k_0 \leq 1/2$, as opposed to $k_0 \leq k_2^*$ in the previous subsection.

The congested initial conditions case $k_0 > 1/2$ is shown in Fig. 7, which indicates that the CS occupancy tends to gridlock shortly after $t = 0$ but then eases back to the equilibrium occupancy k_2^* . We have verified that the effect of the initial condition for ξ_0 (=1 km in the figure) is only transient, and the solution quickly converges to the solution when $\xi_0 = 0^+$.

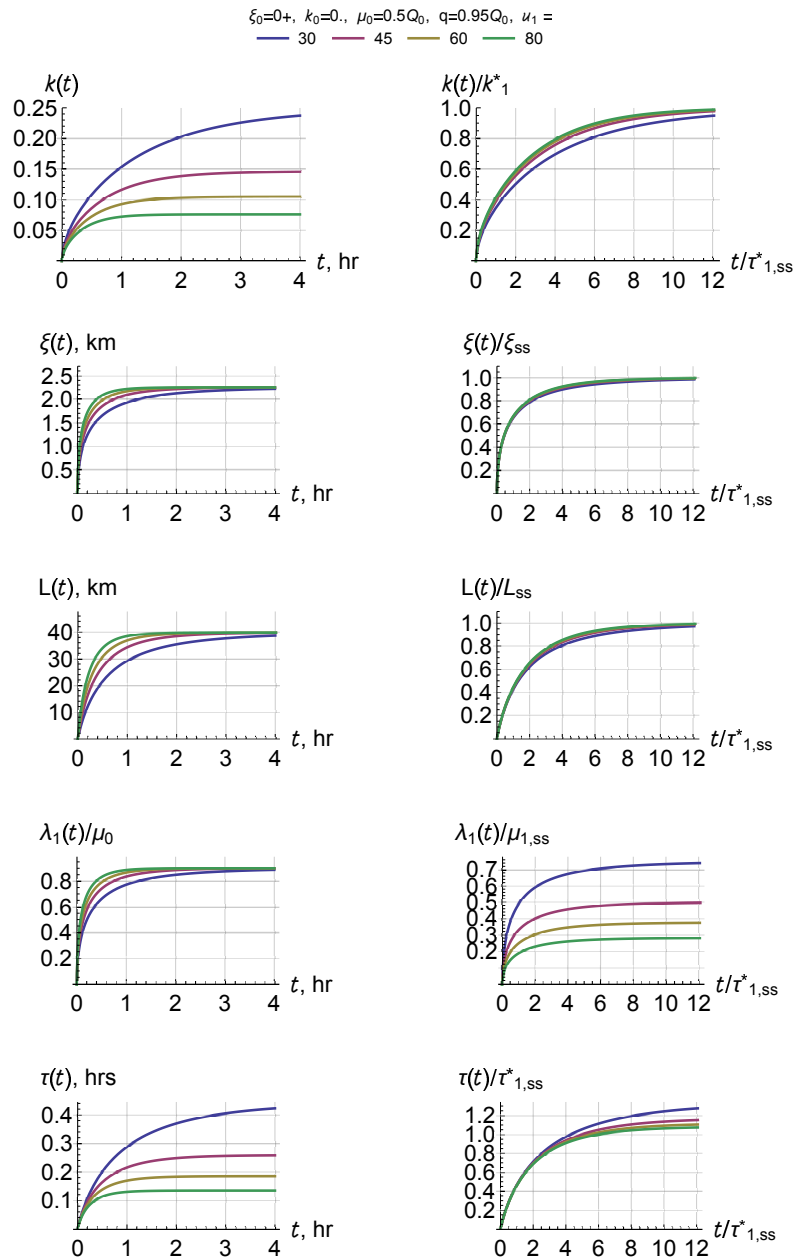


Fig. 6. Freeway vs NMFD, variable network length model. Evolution of various quantities in the case of a constant demand $\lambda(t) \equiv q$ for 4 different free-flow CS speeds μ_1 , and for empty CS initial conditions. First column: regular units; second column: dimensionless. We took: number of freeway lanes = 3, $Q_0 = 2500$ veh/hr/ln, $\kappa = 150$ veh/km/ln, $\gamma = 4$, $\delta = .1$ km, $\phi = 1500$ veh/hr/km.

5. Discussion

We analyzed two formulations of the dynamic user equilibrium on a freeway with a fixed capacity and the surrounding city-streets network, modeled with an NMFD. The traditional approach of constant network and trip lengths

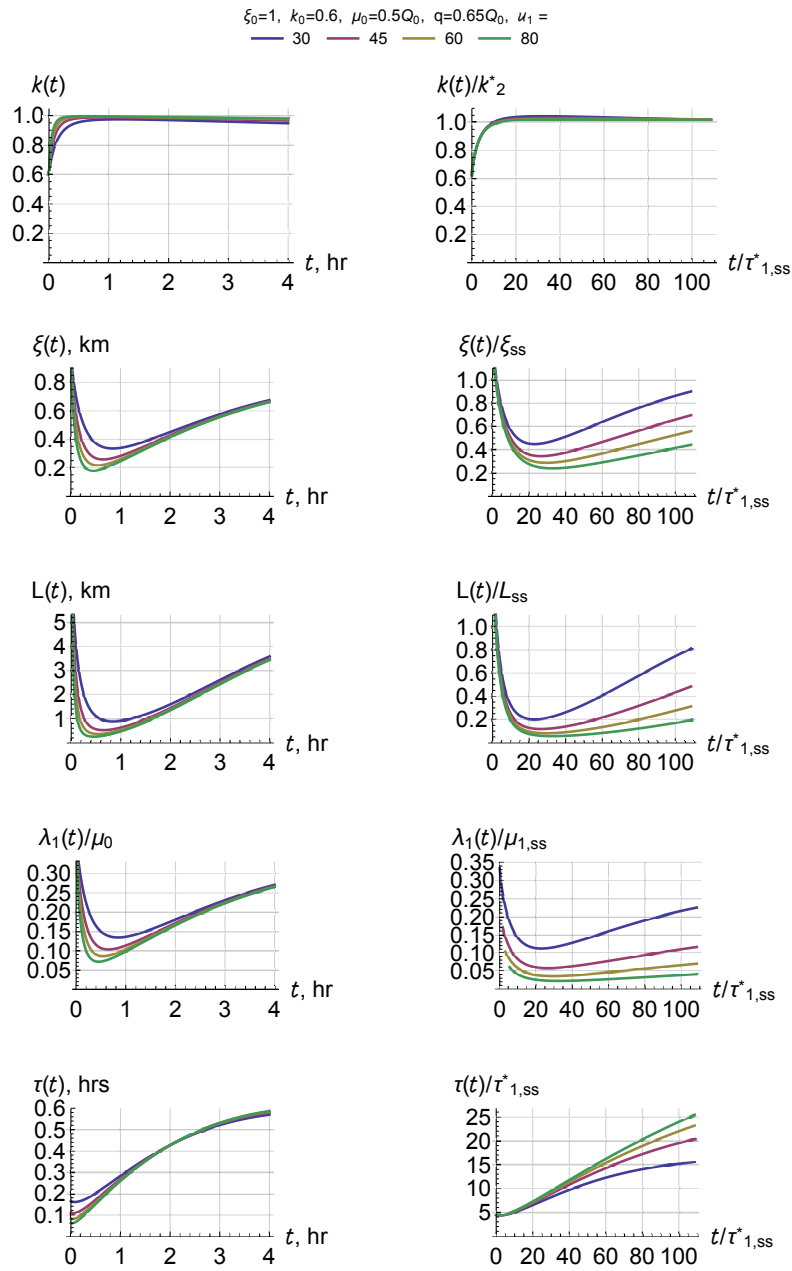


Fig. 7. Freeway vs MFD, variable network length model. Similar to Fig. 6 but with congested initial conditions.

for the NMFD was amenable for analytical solution in the constant total demand case, which could be used as building block for more general demand patterns. When network and trip lengths are allowed to vary to reflect that off-ramp capacities are finite, analytical solutions become impossible, but numerical solutions reveal that the system shares many similarities the constant length model. The main difference being that in the varying length model gridlock does

not happen, and that the steady-state solution is independent of surface network parameters. In all cases we find that convergence rates are very similar when time is expressed in units of the NMF free-flow travel time.

Our results can be extended in the number of directions. It is expected that formulations for the trip length other than (25) might lead to different dynamics. Also, queue spillbacks are not considered here. As argued in Laval (2009), these should not be a problem for the freeway queue because the information tends to travel faster than the shock wave, and since chances are that the freeway bottleneck capacity is higher than the off-ramp capacity, off-ramps located inside the freeway queue would not be starved, i.e. able to discharge at capacity. Spillbacks from off-ramp queues could be a problem if they starve the freeway bottleneck, however. These and other extensions are being studied by the authors.

Acknowledgments.

This study has received funding from NSF research project # 1562536, and from the European Research Council (ERC) under the European Unions Horizon 2020 research and innovation program (grant agreement No 646592 MAGNUM project).

Appendix A. Expression $k(t)$ in section 2 for a few special cases.

Exponential demand function with $\beta = 1/2$, $q_1 = 0$ and arbitrary k_0, q_0 :

$$k(t) = \frac{e^{-t} (\rho \sin(a) + 2 \sqrt{\rho} k_0 \cos(a))}{2 \sqrt{\rho} \cos(a) - 4k_0 \sin(a)}, \quad (\text{A.1})$$

where t is measured in units of $2t^*$, $\rho = q_0/\mu$ and $a = (1 - e^{-t}) \sqrt{\rho}\beta$.

Exponential demand function with $\beta = 3/2$, $q_1 = 0$ and arbitrary k_0, q_0 :

$$k(t) = \frac{3\rho e^{-t} (\sin(a) (3\rho - 4k_0) + 6k_0 \sqrt{\rho} \cos(a))}{2(3 \sqrt{\rho} \cos(a) (4k_0 (e^t - 1) + 3\rho) - 2 \sin(a) (9k_0\rho + e^t (4k_0 - 3\rho)))}, \quad (\text{A.2})$$

where t is measured in units of $2t^*$ and ρ, a same as above.

Exponential demand function with $\beta = 1/(2\sqrt{(1-\rho)})$, $q_0 = 0$ and arbitrary k_0, q_1 :

$$k(t) = \frac{\sinh(a) (k_1^* (k_1^* - 4k_0) - \rho e^{-t}) + 2 \sqrt{\rho} \cosh(a) (k_1^* (1 - e^{-t}) + k_0 e^{-t})}{2 \sqrt{\rho} \cosh(a) - 4 \sinh(a) (k_0 - k_1^*)}, \quad (\text{A.3})$$

where t is measured in units of $2t^*$, $\rho = q_1/\mu$ and $a = \rho (1 - e^{-t}) / (2 \sqrt{(1-\rho)\rho})$.

Logistic demand function with $q_0 = 0$ and arbitrary k_0, q_1 :

$$k(t) = \frac{\rho \beta e^{t/\beta} (H e^t (4(\beta - 1)B (k_0 - 1) + \rho \beta G) + 4(\beta + 1)DF k_0 - \rho \beta IF) - 4A(\beta - 1) (4(\beta + 1)Dk_0 - \rho \beta I)}{4(-a(\beta + 1)C e^t (4(\beta - 1)B (k_0 - 1) + \rho \beta G) - A(\beta - 1) (4(\beta + 1)Dk_0 - \rho \beta I))} \quad (\text{A.4})$$

where t is measured in units of t^* , $\rho = q_1/\mu$ and: $a = k_1^*\beta$, $b = k_2^*\beta$, $A = \mathcal{W}[a, -b, 1 - \beta, -e^{t/\beta}]$, $B = \mathcal{W}[a, -b, 1 - \beta, -1]$, $C = \mathcal{W}[a, -a, 1 + \beta, -e^{t/\beta}]$, $D = \mathcal{W}[a, -a, 1 + \beta, -1]$, $I = \mathcal{W}[1 + a, 1 + b, 2 + \beta, -1]$, $F = \mathcal{W}[1 - a, 1 - b, 2 - \beta, -e^{t/\beta}]$, $G = \mathcal{W}[1 - a, 1 - b, 2 - \beta, -1]$, $H = \mathcal{W}[1 + a, 1 + b, 2 + \beta, -e^{t/\beta}]$, and $\mathcal{W}[\cdot]$ is the Hypergeometric 2F1 function.

References

- Aboudolas, K., Geroliminis, N., Sep. 2013. Perimeter and boundary flow control in multi-reservoir heterogeneous networks. *Transportation Research Part B: Methodological* 55, 265–281.
URL <http://linkinghub.elsevier.com/retrieve/pii/S0191261513001185>
- Ampountolas, K., Zheng, N., Geroliminis, N., Oct 2014. Robust control of bi-modal multi-region urban networks: An lmi optimisation approach. In: *Intelligent Transportation Systems (ITSC), 2014 IEEE 17th International Conference on*. pp. 489–494.
- Amott, R., 2013. A bathtub model of downtown traffic congestion. *Journal of Urban Economics* 76, 110–121.
URL <http://www.sciencedirect.com/science/article/pii/S0094119013000107>
- Daganzo, C. F., Jan. 2007. Urban gridlock: Macroscopic modeling and mitigation approaches. *Transportation Research Part B: Methodological* 41 (1), 49–62.
URL <http://www.sciencedirect.com/science/article/B6V99-4JWFGNC-2/1/4659a928fcc742053a9587464572f409>
- Daganzo, C. F., Knoop, V. L., 2016. Traffic flow on pedestrianized streets. *Transportation Research Part B: Methodological* 86, 211 – 222.
- Daganzo, C. F., Lehe, L. J., 2015. Distance-dependent congestion pricing for downtown zones. *Transportation Research Part B: Methodological* 75, 89 – 99.
- Fosgerau, M., 2015. Congestion in the bathtub. *Economics of Transportation* 4 (4), 241–255.
URL <http://www.sciencedirect.com/science/article/pii/S2212012215000398>
- Geroliminis, N., Daganzo, C. F., 2007. Macroscopic modeling of traffic in cities. In: *Transportation Research Board 86th Annual Meeting*. 07-0413. Washington DC.
- Geroliminis, N., Sun, J., 2011. Properties of a well-defined macroscopic fundamental diagram for urban traffic. *Transportation Research Part B* 45, 605–617.
- Godfrey, J. W., 1969. The mechanism of road network. *Traffic Engineering and Control* 7 (11), 323–327.
- Haddad, J., Geroliminis, N., 2012. On the stability of traffic perimeter control in two-region urban cities. *Transportation Research Part B: Methodological* 46 (9), 1159–1176.
URL <http://www.sciencedirect.com/science/article/pii/S0191261512000641>
- Hajiahmadi, M., Knoop, V., De Schutter, B., Hellendoorn, H., Oct 2013. Optimal dynamic route guidance: A model predictive approach using the macroscopic fundamental diagram. In: *Intelligent Transportation Systems - (ITSC), 2013 16th International IEEE Conference on*. pp. 1022–1028.
- Knoop, V. L., Hoogendoorn, S. P., 2014. Network transmission model: a dynamic traffic model at network level. In: *Transportation Research Board 93rd Annual Meeting*. 14-1104. Washington DC.
- Kouvelas, A., Saeedmanesh, M., Geroliminis, N., 2016. Enhancing feedback perimeter controllers for urban networks by use of online learning and data-driven adaptive optimization. In: *Transportation Research Board 95th Annual Meeting*. 16-3873. Washington DC.
URL <https://trid.trb.org/view/1393432>
- Lamotte, R., Geroliminis, N., 2016. The morning commute in urban areas: Insights from theory and simulation. In: *Transportation Research Board 95th Annual Meeting*. 16-2003. Washington DC.
URL <https://trid.trb.org/view/1392730>
- Laval, J., Castrillon, F., 2015. Stochastic approximations for the macroscopic fundamental diagram of urban networks. *Transportation Research Part B* 81 (3), 904–916, (also in *21th International Symposium of Transportation and Traffic Theory*).
- Laval, J. A., 2009. Graphical solution and continuum approximation for the single destination dynamic user equilibrium problem. *Transportation Research Part B* 43 (1), 108–118.
- Laval, J. A., Chilukuri, B. R., 2016. Symmetries in the kinematic wave model and a parameter-free representation of traffic flow. *Transportation Research Part B: Methodological* 89, 168 – 177.
- Leclercq, L., Chiabaut, N., Trinquier, B., 2014. Macroscopic fundamental diagrams: A cross-comparison of estimation methods. *Transportation Research Part B: Methodological* 62 (0), 1 – 12.
- Leclercq, L., Geroliminis, N., 2013. Estimating mfd in simple networks with route choice. *Transportation Research Part B: Methodological* 57, 468–484.
URL <http://www.sciencedirect.com/science/article/pii/S0191261513000878>
- Leclercq, L., Parzani, C., Knoop, V. L., Amourette, J., Hoogendoorn, S. P., 2015. Macroscopic traffic dynamics with heterogeneous route patterns. *Transportation Research Part C: Emerging Technologies* 55, 292–307.
URL <http://www.sciencedirect.com/science/article/pii/S0968090X15001783>
- Lighthill, M. J., Whitham, G., 1955. On kinematic waves. I Flow movement in long rivers. II A theory of traffic flow on long crowded roads. *Proceedings of the Royal Society of London* 229 (A), 281–345.
- Mahmassani, H., Williams, J. C., Herman, R., 1984. Investigation of network-level traffic flow relationships: Some simulation results. *Transportation Research Record*, 121–130 Cited By 27.
- Mahmassani, H., Williams, J. C., Herman, R., July 1987. Performances of urban traffic networks. In: *10th International Symposium on Transportation and Traffic Theory*. pp. 1–20.
- Mahmassani, H. S., Saberi, M., Zockaie, A., 2013. Urban network gridlock: Theory, characteristics, and dynamics. *Transportation Research Part C: Emerging Technologies* 36, 480 – 497.
- Mariotte, G., Leclercq, L., Laval, J. A., 2017. Macroscopic urban dynamics: Analytical and numerical comparisons of existing models. *Transportation Research Part B: Methodological* 101, 245 – 267.
- Richards, P. I., 1956. Shockwaves on the highway. *Operations Research* (4), 42–51.

- Saberi, M., Mahmassani, H., 2013. Empirical characterization and interpretation of hysteresis and capacity drop phenomena in freeway networks. *Transportation Research Record* 2391, 44–55.
- Teschl, G., 2010. *Differential equations and dynamical systems*. Graduate Studies in Mathematics. American Mathematical Society, Providence, Rhode Island, autre tirage : 2006.
- Wang, P., Wada, K., Akamatsu, T., Hara, Y., 2015. An empirical analysis of macroscopic fundamental diagrams for sendai road networks. *Interdisciplinary Information Sciences* 21 (1), 49–61.
- Yildirimoglu, M., Geroliminis, N., 2014a. Approximating dynamic equilibrium conditions with macroscopic fundamental diagrams. *Transportation Research Part B: Methodological* 70, 186 – 200.
- Yildirimoglu, M., Geroliminis, N., 2014b. Approximating dynamic equilibrium conditions with macroscopic fundamental diagrams. In: *Transportation Research Board 93rd Annual Meeting*. 14-0709. Washington DC.
- Yildirimoglu, M., Ramezani, M., Geroliminis, N., 2015. Equilibrium analysis and route guidance in large-scale networks with {MFD} dynamics. *Transportation Research Part C: Emerging Technologies* 59, 404–420.
URL <http://www.sciencedirect.com/science/article/pii/S0968090X15001813>